Available online at https://jcst.rsu.ac.th
Formerly Rangsit Journal of Arts and Sciences (RJAS)

Journal of Current Science and Technology, January-June 2018 JCST Vol. 8 No. 1, pp. 1-9

ISSN 2630-0583 (Print)/ISSN ….-…. (Online)

A new three-dimensional zinc(II)−barium(II) coordination polymer based on trimesic acid and imidazole ligands: synthesis, structure and properties

Natthakorn Phadungsak[1], Supakorn Boonyuen[2], Darunee Sertphon[3], Winya Dungkeaw[4], Filip Kielar[5] and Kittipong Chainok[1]*

[1]Materials and Textile Technology, Faculty of Science and Technology, Thammasat University, Patumthani 12121, Thailand
[2]Department of Chemistry, Faculty of Science and Technology, Thammasat University, Patumthani 12121, Thailand
[3]Department of Chemistry, Faculty of Science, Rangsit University, Patumthani 12000, Thailand
[4]Department of Chemistry, Faculty of Science, Mahasarakham University, Mahasarakham 44150, Thailand
[5]Department of Chemistry, Faculty of Science, Naresuan University, Phitsanulok 65000, Thailand

*Corresponding author; Email: kc@tu.ac.th

Submitted 23 April 2018; accepted in final form 20 June 2018
Available online 29 June 2018

Abstract

A new zinc(II)–barium(II) bimetallic coordination polymer, $[BaZn_2(TMA)_2(Im)_2]$ (**1**), has been synthesized by hydrothermal reaction of zinc*(*II*)* acetate, barium*(*II*)* acetate, trimesic acid *(*H_3TMA*)*, and imidazole *(*Im*)*, and was characterized by single-crystal X-ray diffraction, powder X-ray diffraction, elemental analysis, thermogravimetric analysis, and infrared and photoluminescence spectroscopy. Single crystal X-ray analysis reveals that compound **1** crystallizes in the centrosymmetric triclinic system with space group *P*-1 and features a dense three-dimensional framework. Compound **1** exhibits intense blue fluorescent emission in the solid state at room temperature and the framework shows remarkable thermal stability up to 460°C.

Keywords: *coordination polymers, crystal structure, photoluminescence, cobalt(II), barium(II), zinc(II)*

1. Introduction

Research of coordination polymers with repeating units extending in one, two, or three dimensions has expanded rapidly in the past two decades because of their intriguing structures and topologies, as well as their potential applications in the fields of magnetism (Batten & Murray, 2003), luminescence (Heine & Müller-Buschbaum, 2013), gas adsorption (Getman, Bae, Wilmer, & Snurr, 2012), sensors (Kreno et al., 2012), non-linear optics (Wang & Pan, 2016), and catalysis (Zhu, Lui, Jiang, & Sun, 2017). Considerable progress has been achieved in the design and application of compounds based on transition or lanthanide metals with a variety of benzene carboxylate ligands such as trimesic acid (Chui, Lo, Charmant, Orpen, & Williams, 1999) and terephthalic acid (Li, Eddaoudi, O'Keeffe, & Yaghi, 1999). However, the field of coordination polymers containing *s*- and *d*-metals has been investigated insufficiently. This is because control over the stoichiometries and structures of these mixed alkali and transition bimetallic complexes is synthetically difficult due to the challenge in manipulating the different coordination sites of the metal cations. Despite the abundance and diversity of the structures of coordination polymers to date, establishing structure-function correlations within these materials still remains a challenging task in the fields of crystal engineering and chemical crystallography. In general, there are various key factors affecting the structural formation, including metal-to-ligand molar ratio, solvent system, concentration of precursors, temperature, time, pH, coordination geometry of metal ions and the coordinative function of the ligands (Lin et al., 2009). Thus, before we are truly able to design and build specifically engineered solid-state architectures, it is important to understand such external factors that govern the crystallization process and the stability of the overall crystals. Here we report a new mixed alkali/transition metals-based coordination polymer with the formula $[BaZn_2(TMA)_2(Im)_2]$ (**1**), which is constructed by using trimesic acid and imidazole under hydrothermal conditions.

2. Objectives

Our academic studies aim to provide a better understanding of the relationships between

the crystallization process and the resulting crystallographic phase by introducing aromatic tricarboxylic acids as main building blocks and using aromatic diamine planar geometry of imidazole as ancillary ligand for the hydrothermal self-assembly synthesis of mixed alkali/transition metals-based coordination polymers.

3. Materials and methods

All chemicals were reagent grade and were used without further purification. Elemental (C, H, N) analysis was determined with a LECO CHNS 932 elemental analyser. FT-IR spectra were recorded on a Perkin-Elmer model Spectrum GX FTIR spectrometer using KBr pellets, in the range of 400–4000 cm^{-1}. Powder X-ray diffraction (PXRD) measurements were carried out on a Bruker D8 ADVANCE X-ray powder diffractometer using Cu Kα (λ = 1.5418 Å). The simulated powder patterns were calculated from single crystal X-ray diffraction data and processed by the free Mercury version 3.5.1 program provided by the Cambridge Crystallographic Data Centre (Macrae, *et al*., 2008). Thermogravimetric analyses (TGA) were carried out using a Metter Toledo TGA/DSC3+ from 30−1000 °C with a heating rate of 10 °C/min, under nitrogen atmosphere. The photoluminescence spectra were measured at room temperature using a Horiba Scientific model FluoroMax-4 spectrofluorometer.

3.1 Synthesis of $[BaZn_2(TMA)_2(Im)_2]$ (**1**)

A mixture of $Ba(CH_3COO)_2$ (64.0 mg, 0.25 mmol), $Zn(CH_3COO)_2{\cdot}2H_2O$, (62.0 mg, 0.25 mmol), H_3TMA (105.0 mg, 0.50 mmol), and Im (69.0 mg, 1.0 mmol) in distilled H_2O (6 mL) was placed in a Teflon lined reactor, stirred at room temperature for 10 min, sealed in a 23 mL stainless steel autoclave, placed in an oven, and then heated to 170°C under autogenous pressure for 48 h. The reaction mixture was cooled to room temperature. After filtration, the product was washed with distilled H_2O, dried in air at room temperature, and isolated as colorless plate-like crystals, yield: 55% based on Zn^{II} source. Anal. calc. for $C_{24}H_{14}BaZn_2N_4O_{12}$: C, 35.22; H, 1.72; N, 6.85%. Found: C, 35.63; H, 1.46; N, 6.72%. FT-IR (KBr, ν/cm^{-1}, s for strong, m medium, w weak): 3340 (w), 3135 (w), 3074 (w), 1614 (s), 1571 (s), 1557 (s), 1537 (s), 1456 (s), 1420 (s), 1370 (s), 1333 (s), 1202 (w), 1178 (w), 1100 (m), 1063 (s), 812 (w), 765 (s), 735 (s), 650 (w), 614 (w), 533 (w).

3.2 X-ray crystallography

A single crystal of **1** with dimensions of 0.25 × 0.20 × 0.08 mm was mounted to the end of a hollow glass fiber. X-ray diffraction data were collected using a Bruker D8 QUEST CMOS and operating at T = 296(2) K. Data were measured using ω and ϕ scans and using Mo-Kα radiation (λ = 0.71073 Å). The total number of runs and images was based on the strategy calculation from the program APEX3 and unit cell indexing was refined using SAINT (V8.38A). Data reduction and scaling were performed using SAINT (V8.38A) and SADABS-2016/2 was used for absorption correction (Bruker, 2016). The structure was solved with the ShelXT structure solution program using combined Patterson and dual-space recycling methods (Sheldrick, 2015*a*). The crystal structure was refined by least squares using ShelXL (Sheldrick, 2015*b*). All non-hydrogen atoms were refined anisotropically. Hydrogen atoms bonded to carbon atoms were placed at calculated positions and refined using a riding model approximation, with C−H = 0.93 (aromatic CH) and with U_{iso}(H) = 1.2U_{eq}(C). The O−H and N−H hydrogen atoms were located in difference Fourier maps but refined with O−H = 0.84 ± 0.01 Å with U_{iso}(H) = 1.5U_{eq}(O) and N−H = 0.86 ± 0.01 Å with U_{iso}(H) = 1.2U_{eq}(N), respectively. A summary of crystal data and structural refinement parameters for compound **1** is given in Table 1. Crystallographic data for compound **1** have been deposited in the Cambridge Crystallographic Data Centre, CCDC number 1510755.

Table 1 Crystal data and structure refinement for compound **1**

Compound	**1**
Crystal data	
CCDC number	1510755
Empirical formula	$C_{24}H_{14}BaN_4O_{12}Zn_2$
Formula weight	818.47
Crystal system, space group	Triclinic, *P*-1
Temperature (K)	296(2)
a (Å)	7.4409(8)
b (Å)	11.2765(12)
c (Å)	15.3526(16)
α, (°)	95.493(4)
β, (°)	97.535(4)
γ (°)	105.267(3)
V (Å^3)	1220.5(2)
Z	2
Radiation type	Mo *K*α (λ = 0.71073 Å)
μ (mm^{-1})	3.63
Crystal size (mm)	0.25 × 0.20 × 0.08
Data collection	
Diffractometer	Bruker D8 QUEST CMOS
Absorption correction	Multi-scan
2θ range for data collection	5.76−55.14
Index ranges	$-8 \le h \le 9$, $-14 \le k \le 14$, $-19 \le l \le 19$
T_{min}, T_{max}	0.674, 0.746
Number of measured reflections	39021
Number of independent reflections	5636
Number of observed [$I > 2\sigma(I)$] reflections	5084
R_{int}, R_{sigma}	0.0574, 0.0327
$(\sin\theta/\lambda)_{max}$ (Å^{-1})	0.651
Data completeness (θmax)	99.9 (θ_{max} = 27.571°)
Refinement	
Final *R* indexes [$F^2 > 2\sigma(F^2)$]	R_1 = 0.0247, wR_2 = 0.0588
Final *R* indexes [all data]	R_1 = 0.0299, wR_2 = 0.0605
Goodness-of-fit on F^2, *S*	1.095
Number of reflections	5636
Number of parameters	396
Number of restraints	2
H-atom treatment	H-atom parameters constrained
$\Delta\rho_{max}$, $\Delta\rho_{min}$ (e Å^{-3})	0.43, −0.85

Computer programs: SAINT v8.37A (Bruker, 2016), SHELXT (Sheldrick, 2015*a*), SHELXL (Sheldrick, 2015*b*), Olex2 (Dolomanov *et al*., 2009).

4. Results and discussion

4.1 Structural description

The single-crystal X-ray analysis reveals that **1** crystallizes in the centrosymmetric triclinic system with the space group *P*-1. The asymmetric unit of **1** contains two crystallographically independent Zn^{II} ions, one Ba^{II} ion, two completely deprotonated TMA^{3-} ligands and two Im ligands. Each Zn^{II} ion adopts four-coordinated distorted tetrahedral geometry completed by three oxygen atoms from three different TMA^{3-} ligands and one nitrogen atom from the Im ligand. The Zn−O bond lengths fall in the range of 1.9449(18)–2.0810(19) Å, and the Zn−N bond lengths are 1.983(2) and 1.989(2) Å for Zn1−N1 and Zn2−N3, respectively. The N−Zn−O and O−Zn−O bond angles fall in the range of 95.80(8) − 132.61(8)°. The Ba^{II} ion is nine-coordinated and bears a tricapped trigonal prism geometry, which is completed by nine oxygen atoms from six different TMA^{3-} ligands. The Ba−O bond lengths are in the range 2.6755(19) − 2.8752(19) Å and the O−Ba−O bond angles are in the range of 45.94(5) − 147.47(6)°. The bond lengths and bond angles around the metal centers in **1** are in accordance with previous reports (Du et al., 2013; Foo, Horike, Duan, Chen, & Kitagawa, 2013).

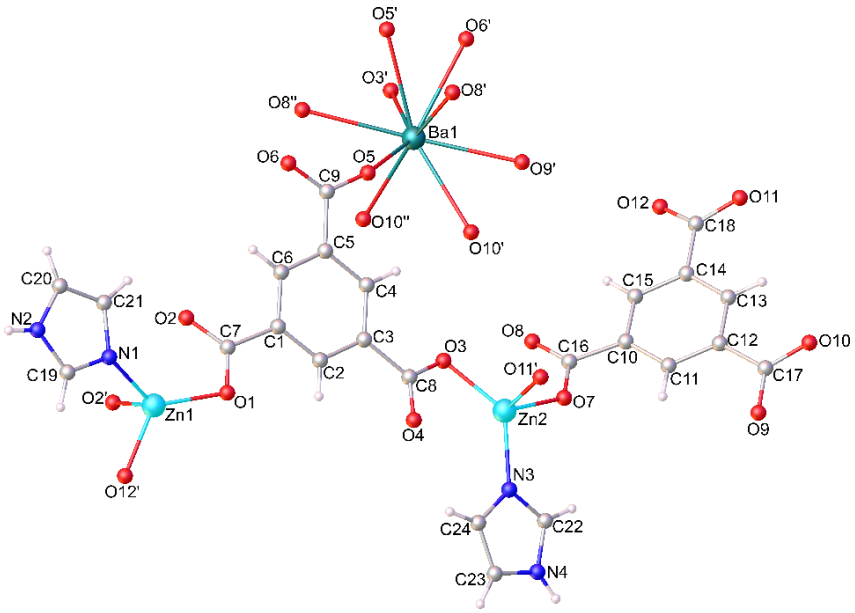

Figure 1 Coordination environment of the metal ion centers in **1**

It is interesting to note that the TMA^{3-} ligand in **1** adopts two different coordination modes, namely, one acts as μ_5-η^1:η^1:η^1:η^1:η^2 mode to connect three Zn^{II} ions and two Ba^{II} ions, and the other one adopts μ_7-η^1:η^1:η^1:η^1:η^2:η^2 mode to link three Zn^{II} ions and four Ba^{II} ions, as depicted in Figure 2. Along the crystallographic *b* axis, the Ba1 ion and its corresponding centrosymmetric $Ba1^{i}$ ion [symmetry code (i): 1−*x*, 1−*y*, 1−z] are connected by four carboxylate groups of the TMA^{3-} ligands in the bridging-chelating and bridging fashions, forming an edge-sharing dinuclear subunit with the Ba···Ba separation of 3.8418(5) Å. Adjacent dinulcear subunits are linked together *via* two carboxylate groups of the TMA^{3-} ligands in the bridging-chelating fashion, giving rise to the formation of a 2D {Ba-TMA} layer structure as shown in Figure 3. The Ba···Ba separation distance between the two dinuclear units is 4.4351(5) Å, whereas the Ba···Ba distance along the TMA^{3-} ligand being ~11.76 Å. The {Ba-TMA} layers are connected to the Zn^{II} ions through carboxylate groups of the TMA^{3-} bridging ligands to form a dense 3D framework, Figure 4. The Im molecules occupy its edges to complete the coordination sphere of the Zn^{II} metal center and further stabilize the 3D network by forming classical N−H···O hydrogen bonds with the carboxylate groups of the TMA^{3-} ligands. A combination of aromatic π−π stacking interactions (Janiak, 2000) involving the TMA^{3-} molecules (centroid to centroid distance = 3.5916(19) Å) and the TMA^{3-}/Im molecules (centroid to centroid distance = 3.8825(17) Å) along with weak C−H···O hydrogen bonds, Table 2, are also observed in the crystal of **1**.

Table 2 Hydrogen-bond geometry (Å, °) for **1**

D−H···*A*	*D*−H	H···*A*	*D*···*A*	*D*−H···*A*
N2−H2···O6^{i}	0.86(1)	2.07(2)	2.876(3)	156(4)
N4−H4···O11^{ii}	0.86(1)	2.39(3)	3.118(4)	142(4)
C10−H10···O9^{iii}	0.93	2.41	3.019(3)	123
C11−H11···O2^{i}	0.93	2.45	3.370(4)	168
C12−H12···O2	0.93	2.47	3.054(3)	121
C16−H16···O3^{iv}	0.93	2.54	3.430(3)	160
C18−H18···O6^{v}	0.93	2.69	3.497(3)	146
C24−H24···O4	0.93	2.46	3.052(4)	121

Symmetry codes: (i) −*x*+3, −*y*+2, −*z*+2; (ii) −*x*−1, −*y*, −*z*+1; (iii) −*x*+1, −*y*+1, −*z*+2; (iv) −*x*, −*y*, −*z*+1; (v) −*x*+1, −*y*+1, −*z*+1.

JCST Vol. 8 No. 1 Jan.-Jun. 2018, pp. 1-9
ISSN 2630-0583 (Print)/ISSN……. (Online)

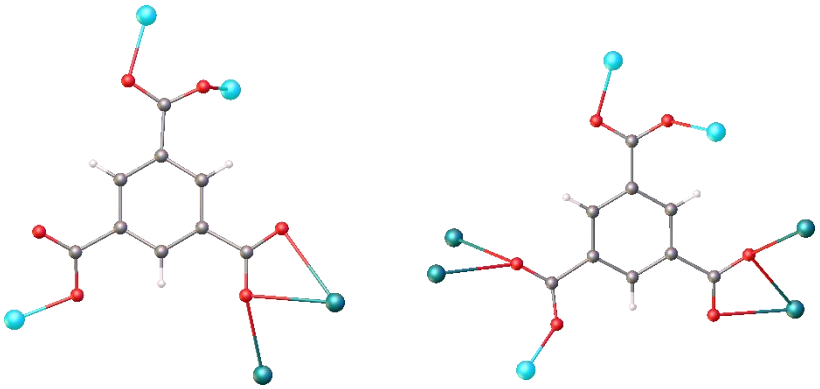

Figure 2 Coordination modes of the TMA^{3-} ligand in **1**.

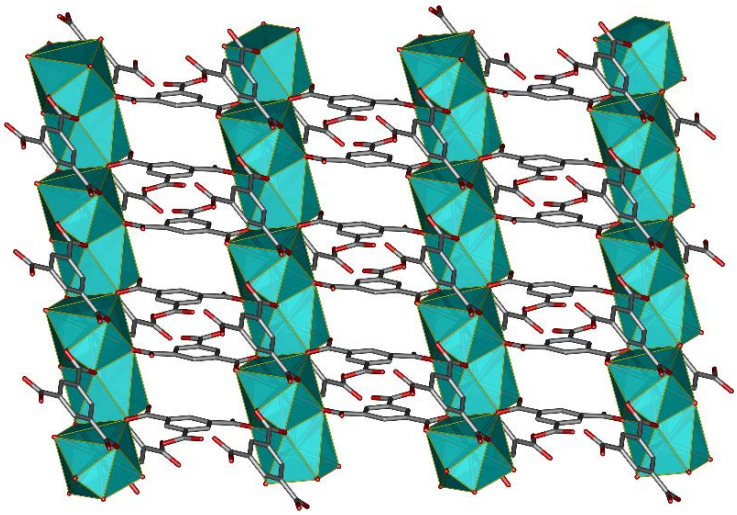

Figure 3 View of the 2D {Ba-TMA} layer structure in **1**.

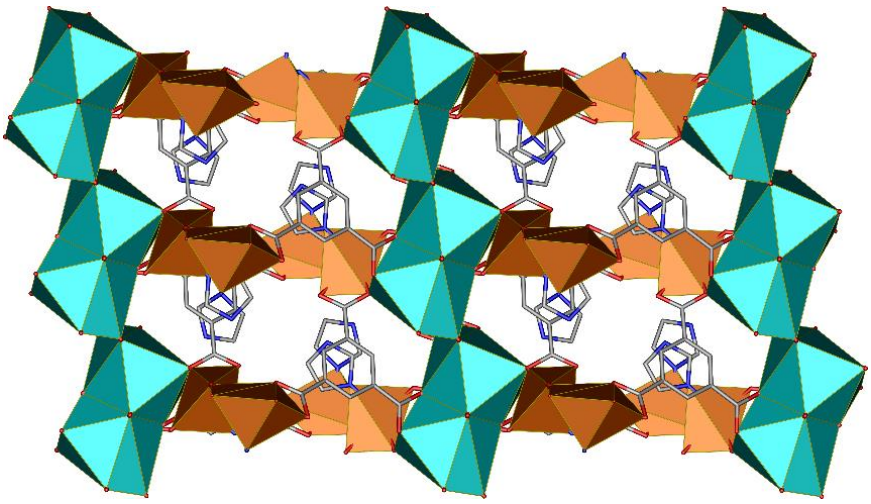

Figure 4 View of the 3D framework in **1**.

4.2 Infrared spectra analysis

The FT-IR spectra of **1** is shown in Figure 5. The absence of the characteristic band at around 1700 cm^{-1} indicates the complete deprotonation of H_3TMA. The characteristic bands of the carboxylate groups within the crystalline solids are presented in the range 1520−1630 cm^{-1} for the asymmetric stretching vibration $\nu_{as}(COO^-)$ and 1310−1450 cm^{-1} for the symmetric stretching vibration $\nu_s(COO^-)$. The presence of NH group in Im has been confirmed by the sharp shoulder band at around 3300−3450 cm^{-1}. Other characteristic bands of the aromatic C=C and the C−H vibration have also been observed around 1400−1600 and 675−1000 cm^{-1}, respectively. The above results are all consistent with the single-crystal X-ray diffraction studies.

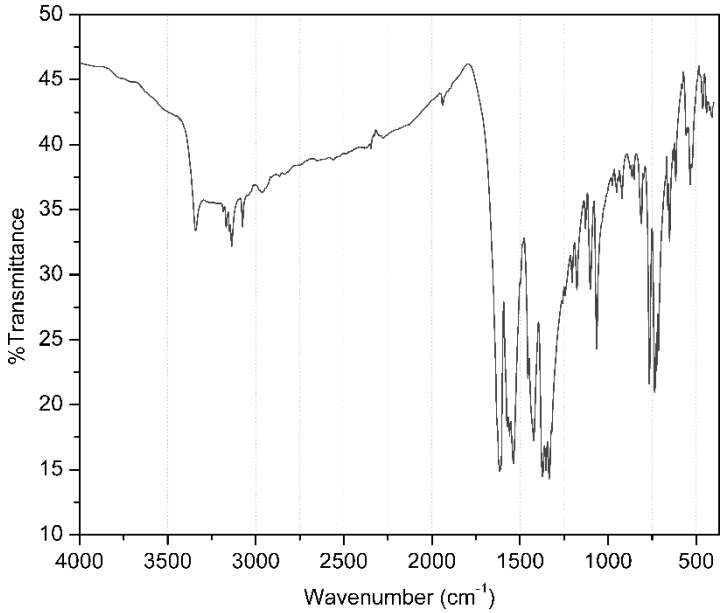

Figure 5 Infrared spectra of **1**.

4.3 PXRD and TG/DTA analyses

Powder X-ray diffraction (PXRD) and thermal gravimetric/differential thermal analyses (TG/DTA) were carried out to investigate the phase purity and stability of the compound. The PXRD patterns for **1** are presented in Figure 6a. The diffraction peaks of both the calculated pattern based on the single-crystal X-ray diffraction and the experimental pattern from the as-synthesized bulk materials match well, indicating the phase purities of compound **1**. The TG/DTA of **1** was performed in a dry nitrogen atmosphere from 30−1000 °C. As can be seen in Figure 6b, the TG/DTA curves of **1** show that there is no weight loss before ~460 °C due to a dense 3D framework and the absence of any coordinated water molecules. The decomposition of the organic TMA^{3-} and Im ligands occurs in the range of 470–525 °C (observed 55.73%, calculated 67.25%) with a collapse of the framework, leaving the final residue of barium zinc oxide ($BaZnO_2$).

4.4 Photoluminescence properties

The luminescence properties of coordination polymers especially those with d^{10} metal ions with nitrogen and carboxylate donor ligands are widely investigated nowadays for potential applications as fluorescence-emitting materials such as light-emitting diodes, LEDs (Xie, *et al.*, 2016). The photoluminescent properties of **1** were therefore investigated, and the results are presented in Figure 6. Irradiation of crystalline samples of **1** with ultraviolet light (λ_{ex} = 290 nm) at room temperature. Intense band in the emission spectra is observed at 420 nm. The free ligand displays an intense luminescent emission with maximum at ~385 nm upon excitation at 365 nm in

the solid state at ambient temperature. The enhancement and red shift ~35 nm (from ~385 to 420 nm) of the emission in **1** compared to that of free ligand might be assigned to a combination of a ligand-to-metal charge transfer (LMCT) process and intraligand emission states (Chang, Zhang, Hu, & Bu, 2009), which may be due to its unique dense 3D framework with π–π stacking interactions between the aromatic rings of the ligands.

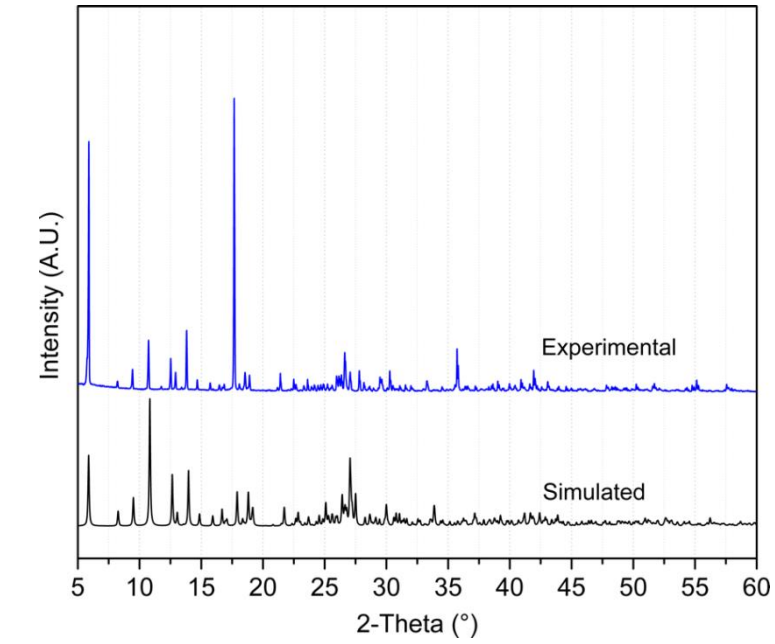

(a)

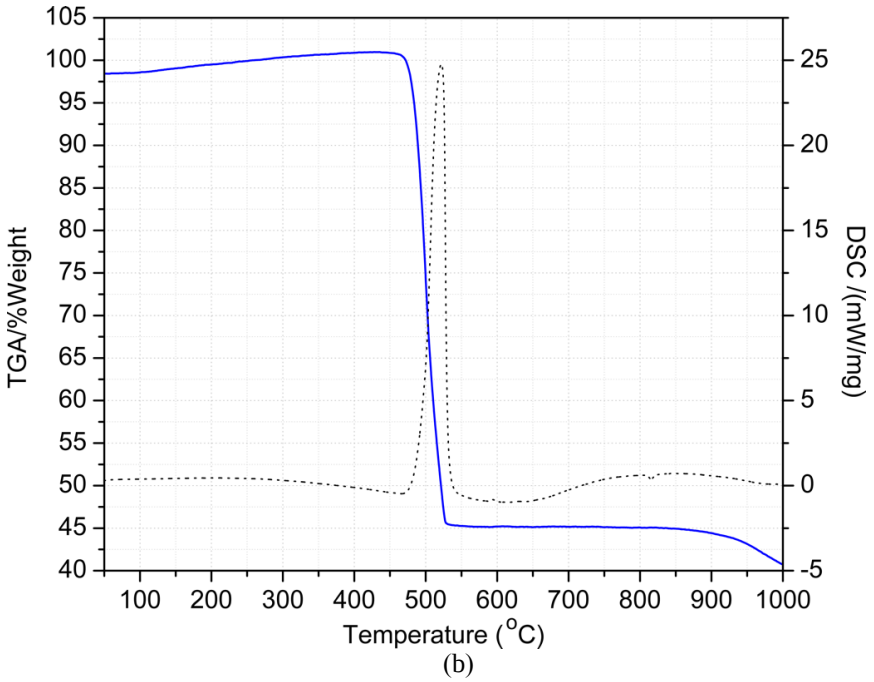

(b)

Figure 6 PXRD patterns simulated from the single crystal X-ray structure and as-synthesized (a) and TG/DTA curve (b) of **1**.

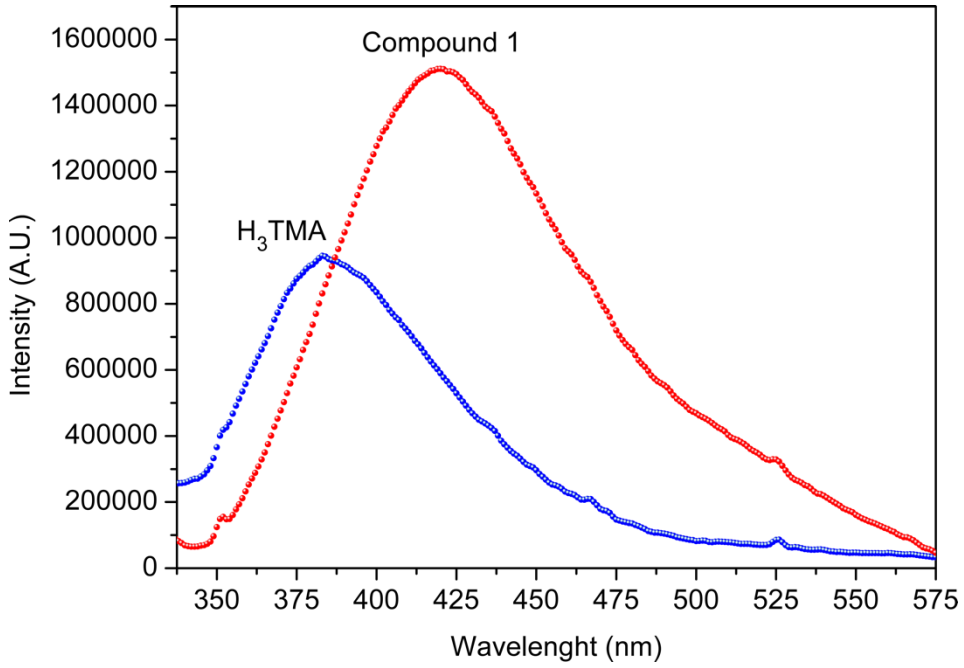

Figure 7 Solid state emission spectra at room temperature of the H_3TMA ligand and **1**

5. Conclusion

We have synthesized and characterized a new mixed alkali metal/transition metal coordination polymer based on benzene tricarboxylate and the neutral *N*-donor ligands. It is evident that the TMA^{3-} ligand has versatile coordination modes to construct high-dimensional framework. The polymeric compound exhibits excellent photoluminescence properties and high thermostability.

6. Acknowledgements

The authors gratefully acknowledge the financial support provided by Thammasat University under the TU Research Scholar, Contract No. 2/6/2558. N. P. thanks the National Research Council of Thailand for financial support.

7. References

Batten, S. R., & Murray, K. S. (2003). Structure and magnetism of coordination polymers containing dicyanamide and tricyanomethanide. *Coordination Chemistry Reviews*, *246*, 103-130. DOI: https://doi.org/10.1016/S0010-8545(03)00119-X

Bruker. (2016). APEX3, SADABS and SAINT. Bruker AXS Inc., Madison, Wisconsin, USA.

Chang, Z., Zhang, A.-S., Hu, T.-L., & Bu, X.-H. (2009). Zn^{II} coordination polymers based on 2,3,6,7-anthracenetetracarboxylic acid: synthesis, structures, and luminescence properties. *Crystal Growth & Design*, *9*(11), 4840-4846. DOI: 10.1021/cg900659r

Chui, S. S.-Y., Lo, S. M.-F., Charmant, J. P. H., Orpen, A. G., & Williams, I. D. (1999). A chemically functionalizable nanoporous material $[Cu_3(TMA)_2(H_2O)_3]_n$. *Science*, *283*, 1148-1150. DOI: 10.1126/science.283.5405.1148

Dolomanov, O. V., Bourhis, L. J., Gildea, R. J., Howard, J. A. K., & Puschmann, H. (2009). OLEX2: a complete structure solution, refinement and analysis program. *Journal of Applied Crystallography*, *42*, 339-341. DOI: 10.1107/S0021889808042726

Du, P., Yang, Y., Yang, J., Liu, Y.-Y., Kan, W.-Q., & Ma, J.-F. (2013). A series of MOFs

based on a tricarboxylic acid and various N-donor ligands: syntheses, structures, and properties. *CrystEngCommunity*, *15*, 6986-7002. DOI: 10.1039/C3CE40828K

Foo, M. L., Horike, S., Duan, J., Chen, W., & Kitagawa, S. (2013). Tuning the dimensionality of inorganic connectivity in barium coordination polymers via biphenyl carboxylic acid ligands. *Crystal Growth & Design*, *13*(7), 2965-2972. DOI: 10.1021/cg4003803

Getman, R. B., Bae, Y.-S., Wilmer, C. E., & Snurr, R. Q. (2012). Review and analysis of molecular simulations of methane, hydrogen, and acetylene storage in metal-organic frameworks. *Chemical Reviews*, *112*(2), 703-723. DOI: 10.1021/cr200217c

Heine, J., & Müller-Buschbaum, K. (2013) Engineering metal-based luminescence in coordination polymers and metal-organic frameworks. *Chemical Society Reviews*, *42*, 9232-9242. DOI: 10.1039/C3CS60232J

Kreno, L. E., Leong, K., Farha, O. K., Allendorf, M., Duyne, R. P. V. & Hupp, J. T. (2012). Metal-organic framework materials as chemical sensors. *Chemical Reviews*, *112*(*2*), 1105-1125. DOI: 10.1021/cr200324t

Janiak, C. (2000). A critical account on π–π stacking in metal complexes with aromatic nitrogen-containing ligands. *Journal of the Chemical Society, Dalton Transactions*, *21*, 3885-3896. http://dx.doi.org/10.1039/B003010O

Li, H., Eddaoudi, M., O'Keeffe, M., & Yaghi, O. M. (1999). Design and synthesis of an exceptionally stable and highly porous metal-organic framework. *Nature*, *402*, 276-279. DOI: 10.1038/46248

Lin, X.-M., Fang, H.-C., Zhou, Z.-Y., Chen, L., Zhao, J.-W., Zhu, S.-Z., & Cai, Y.-P. (2009). Temperature- and solvent-controlled dimensionality in a zinc 6-(1*H*-benzoimidazol-2-yl)pyridinecarboxylate system. *CrystEngCommunity*, *11*, 847-854. DOI: 10.1039/B819800D

Macrae, C. F., Bruno, I. J., Chisholm, J. A., Edgington, P. R., McCabe, P., Pidcock, E., Rodriguez-Monge, L., Taylor, R., van de Streek, J., & Wood, P. A. (2008). Mercury CSD 2.0 - new features for the visualization and investigation of crystal structures. *Journal of Applied Crystallography*, *41*, 466-470. DOI: https://doi.org/10.1107/S0021889807067908

Sheldrick, G. M. (2015*a*). SHELXT - Integrated space-group and crystal-structure determination. *Acta Crystallographica Section A: Foundations and Advances*, *71*(part 1), 3-8. DOI: 10.1107/S2053273314026370

Sheldrick, G. M. (2015*b*). Crystal structure refinement with SHELXL. *Acta Crystallographica Section C: Structural Chemistry*, *71*, 3-8. DOI: 10.1107/S2053229614024218

Wang, Y., & Pan, S. (2016). Recent development of metal borate halides: Crystal chemistry and application in second-order NLO materials. *Coordination Chemistry Reviews*, *323*, 15-35. DOI: https://doi.org/10.1016/j.ccr.2015.12.008

Xie, W., He, W.-W., Du, D.-Y., Li, S.-L., Qin, J.-S., Su, Z.-M., . . . Lan, Y.-Q. (2016). A stable Alq3@MOF composite for white-light emission. *Chemical Communications*, *52*, 3288-3291. DOI: 10.1039/C5CC08703A

Zhu, L., Lui, X.-Q., Jiang, H.-L., & Sun, L.-B. (2017). Metal-organic frameworks for heterogeneous basic catalysis. *Chemicals Reviews*, *117*(12), 8129-8176. DOI: 10.1021/acs.chemrev.7b00091